Received: 11 May 2024 | Accepted: 29 September 2024

DOI: 10.1002/prp2.70025

ORIGINAL ARTICLE

Study on the mechanism of echinacoside in preventing and treating hypoxic pulmonary hypertension based on proteomic analyses

Xiangyun Gai[1] | Qingqing Xia[1] | Hongmai Wang[1] | Hongtao Bi[2] | Jinyu Wang[1] | Yuefu Zhao[1]

[1]Department of Pharmacy, Qinghai Minzu University, Xining, China

[2]Qinghai Provincial Key Laboratory of Tibetan Medicine Pharmacology and Safety Evaluation, Northwest Institute of Plateau Biology, Chinese Academy of Science, Xining, China

Correspondence
Xiangyun Gai, Department of Pharmacy, Qinghai Minzu University, Xining, China.
Email: 2015002@qhmu.edu.cn

Funding information
Kunlun Talents and High-level Innovative Entrepreneurship Program of Qinghai Province, Grant/Award Number: 2020; Application Foundation Project grant of Qinghai Province, China, Grant/Award Number: 2020-ZJ-703

Abstract

Hypoxic pulmonary hypertension (HPH), a chronic condition affecting the cardiopulmonary system, has high mortality. Echinacoside (ECH) is a phenylethanoid glycoside, which is used to ameliorate pulmonary vascular remodeling and pulmonary vasoconstriction in rats. Accordingly, we aimed to explore the mechanism of ECH in preventing and treating HPH. Sprague Dawley rats were housed in a hypobaric hypoxia chamber for 28 days to obtain the HPH model. The experimental rats were randomly allocated into the following several groups: normoxia group, chronic hypoxia group, and ECH group. The therapeutic results of ECH (10, 20, and 40 mg/kg) showed that ECH reduced mPAP, Hb, Hct, and RVHI in HPH rats. Then this work employed label-free quantitative proteomic analysis, western blotting, and RT-PCR to investigate the mechanism by which ECH prevents HPH. The results found that in the chronic hypoxia group, the levels of ACSL1, COL6A1, COL4A2, COL1A1, and PC increased compared to the normoxia group. However, the opposite effect was observed in the chronic hypoxia group treated with ECH. The study indicates that the administration of ECH may slow the pathological progression of HPH by suppressing the inflammatory response, inhibiting smooth muscle cell proliferation, and minimizing the deposition of extracellular matrix.

KEYWORDS
cell proliferation, echinacoside, hypoxic pulmonary hypertension, inflammation, proteomics

Abbreviations: ACSL1, Acyl-CoA Synthetase Long-Chain Family Member 1; COL1A1, Collagen alpha-1 (I) chain; COL4A2, Collagen alpha-2 (IV) chain; COL6A1, Collagen alpha-1 (VI) chain; ECH, echinacoside; ECM, extracellular matrix; GAPDH, glyceraldehyde 3-phosphate dehydrogenase; Hb, hemoglobin; Hct, hematocrit; HPH, hypoxic pulmonary hypertension; JNK, c-Jun N-terminal kinase; LA, lumen area; LV, left ventricle; mPAP, mean pulmonary artery pressure; NF-κB, nuclear factor-κB; PASMCs, pulmonary artery smooth muscle cells; PC, Pyruvate carboxylase; PH, pulmonary hypertension; RBC, red blood cell; ROS, reactive oxygen species; RV, right ventricle; RVHI, right ventricle hypertrophy index; WA, wall area; WT, wall thickness.

Xiangyun Gai and Qingqing Xia should be considered as joint first authors.

1 | INTRODUCTION

Hypoxic pulmonary hypertension (HPH) is a cardiovascular disease caused by chronic hypoxia. The disease is characterized by long-term pressure increases within pulmonary arteries resulting from vascular remodeling and pulmonary arterial vasoconstriction. Excessive proliferation within pulmonary microvascular endothelial cells together with pulmonary artery smooth muscle cells (PASMCs) results in pulmonary vasculature remodeling.[1,2] The condition known as HPH is associated with a significant mortality rate, and if left untreated, the affected individuals may get irreversible right heart failure as a consequence. Nowadays, HPH has seriously threatened the health of residents in high-altitude areas.[3] While several medications have been identified that mitigate HPH through their vasodilatory properties, few interventions have been discovered thus far that may successfully reverse vascular remodeling and disease progression.[4]

Echinacoside (ECH) is a phenylethanoid glycoside molecule derived from the Tibetan herb *Cistanche tubulosa* and *Lagotis brevituba Maxim* (Figure 1). It serves as the primary bioactive constituent in *C. tubulosa*.[5,6] Prior research has demonstrated that ECH shows various pharmacological activities, like antioxidative, anti-tumorigenic, neuroprotective, and anti-inflammatory properties.[5,7] The antiproliferative impact of ECH on PASMCs has been demonstrated in earlier studies conducted by our research group.[8] Additionally, ECH induces relaxation of the pulmonary artery by reducing intracellular Ca^{2+} levels. Moreover, it facilitated rat pulmonary artery relaxation by activating NO-cGMP-PKG-BK_{Ca} channels and K^+ channels.[9] In further research, we found that ECH can effectively reduce the average pulmonary artery pressure in HPH rats and improve the right ventricular failure in rats by regulating the function of pulmonary artery endothelium and smooth muscle layer and improving pulmonary artery remodeling. While it has been shown that ECH may impede HPH by suppressing the proliferation of PASMCs and promoting vasodilation, the precise mechanism behind its impact remains uncertain. The alterations in protein expression can provide insights into the functionality and temporal changes within cells.[10] Proteomics is employed as a pioneering approach to discover novel biomarkers to diagnose, predict, and identify disease targets. This method enables the examination of the proteome of a specific cell, tissue, or organism.[11] Therefore, we utilize the label-free quantification technique in proteomics to clarify the specific mechanism by which ECH improves HPH, by detecting the protein content in samples and analyzing the differences in the expression of the same protein among multiple samples.

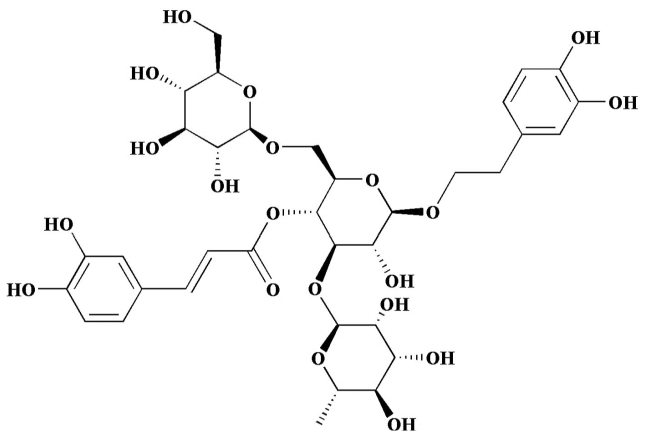

FIGURE 1 Chemical structure of echinacoside.

2 | MATERIALS AND METHODS

2.1 | Experimental animals

The Sprague Dawley (SD) rats employed for this investigation were male, 8 weeks old, weighing 250–300 gm, obtained from Dilepu Bioscience and Technology Medical (Xi'an, China). All animals were treated in accordance with the Guide for the Care and Use of Laboratory Animals, and the treatment was approved by the Experimental Animal Welfare Ethics Review Committee of the Northwest Institute of Plateau Biology, Chinese Academy of Sciences. All efforts were made to lessen the suffering experience of each animal involved in this study.

2.2 | Drugs and reagents

High-performance liquid chromatography grade ECH (170307) with 98% purity was acquired by Beijing Century Aoke Biotechnology (Beijing, China). The primary antibodies used in western blotting assay includes rabbit anti-COL1A1 (BA0325; 1:300 dilution; BOSTER®, Wuhan, China), rabbit anti-ACSL1 (ab177958; 1:1000 dilution; Abcam, Cambridge, UK), rabbit anti-PC (ab128952; 1:1000 dilution; Abcam, Cambridge, UK), rabbit anti-COL6A1 (CSB-PA005751; 1:500 dilution; CUSABIO®, Wuhan, China) and rabbit anti-COL4A2 (BA3626; 1:500 dilution; BOSTER®, Wuhan, China).

2.3 | Treatment of ECH in preventing HPH

The experimental rats were randomly allocated into three groups: the normoxia group, which constituted the control group (group 1, $n=8$); the chronic hypoxia group, which was the disease model group (group 2, $n=8$); and the ECH (30 mg/kg) group (group 3, $n=8$). The rats from group 1 were raised in normoxic conditions. The latter groups (groups 2 and 3) were raised for 28 days within a hypobaric hypoxia chamber (DYC3000 type) (Fenglei, Guizhou, China) with a simulated altitude being 5000 m. The animals in group 3 received ECH once daily via intraperitoneal injection for 28 days (Figure 2A).

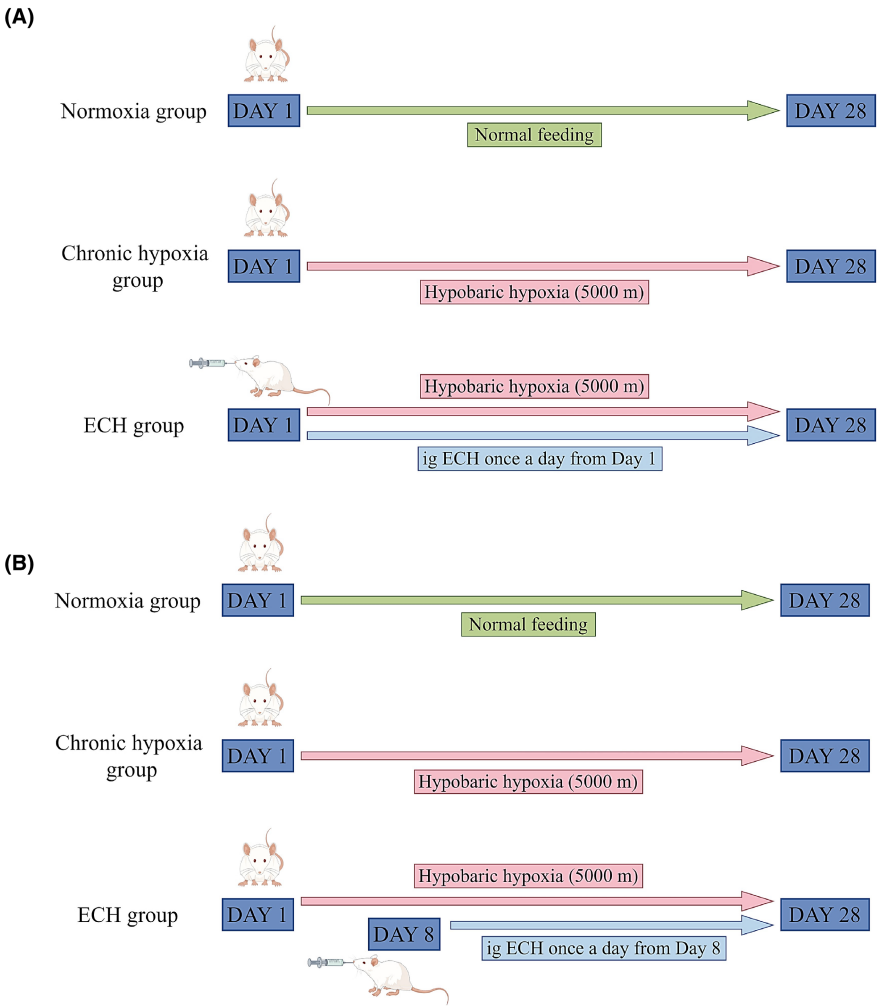

FIGURE 2 Timeline of prevention of hypoxic pulmonary hypertension by ECH (A) and treatment of hypoxic pulmonary hypertension by ECH (B).

It is important to note that the first dosage of ECH was provided concurrently with the initiation of hypoxia.

2.4 | Treatment of ECH in treating HPH

The experimental rats were randomly allocated into five groups: the normoxia group ($n=10$); the chronic hypoxia group ($n=10$); the ECH (10 mg/kg) group ($n=10$); the ECH (20 mg/kg) group ($n=10$); and the ECH (40 mg/kg) group ($n=10$). The ECH was administered on the 8th day after a simulated altitude of 5000 m and lasted for 21 days (Figure 2B). After the administration, the rats received intra-peritoneal sodium pentobarbital administration (dosage range = 40–60 mg/kg) to induce anesthesia. The technique employed for assessing PAP involves the utilization of the right cardiac catheterization. MP100 pressure signal acquisition equipment (Biopac, USA) monitored mean pulmonary artery pressure (mPAP) concurrently with the intubation process. After opening the thoracic cavity of the rats, the right ventricle (RV) was isolated, and then the rats were euthanized. The RV hypertrophy index (RVHI) is calculated by the wet-to-weight ratio of RV to left ventricle (LV) plus interventricular septum (SP). BC5000vet automatic hematocrit analyzer (Mindray, Shenzhen, China) was used to determine hemoglobin (Hb), hematocrit (Hct), and red blood cells (RBC).

2.5 | Morphometric analysis of lung tissues

A 10% (wt./vol.) concentration of formalin solution was used to preserve the apex of the left lung specimen. It was then sliced into sections with a thickness of 4 μm via the RM2265 paraffin microtome (Leica, Germany), and 10 slices were cut continuously. Hematoxylin and eosin (H&E) staining was applied to the sections for morphometric analysis to assess the degree of pulmonary artery remodeling. An optical microscope (Olympus Corporation, Shinjuku, Japan) was used to visually document and capture images of the morphological alterations occurring in the pulmonary arterioles. Image-pro Plus 6.0 software was used to measure the external diameter, wall thickness (WT), wall area, lumen area, and total wall area of complete and clear vascular cross-sections, recording 5–7 values for each slice. The ratios of the wall thickness/external diameter (WT%), wall area/total wall area (WA%), and lumen area/total wall area (LA%) were calculated as indices of pulmonary vascular morphology for further statistical analysis.

2.6 | Label-free quantification technique

Label-Free Quantification Technique analyzed the preventive effect of ECH (30 mg/kg) on HPH rats. Protein was extracted from lung tissue after anesthetizing rats with 7% chloral hydrate. Protein digestion was then conducted by adding 100 μL of a 50 mM ammonium bicarbonate (NH_4HCO_3) solution with the sequencing-grade modified trypsin (Promega) at a ratio of 1:50. The mixture was then incubated at a temperature of 37°C overnight. The separation of peptides was performed using the Dionex Ultimate 3000 system. Afterward 10 fractions were collected, dried by vacuum, and ready for data-dependent acquisition (DDA). The experimental setup employed a Q-Exactive HF-X mass spectrometer combined with nanoLC Easy-nLC 1000 (Thermo Fisher Scientific, USA) for conducting DDA and data-independent acquisition studies. The area of each protein peak is expressed by the relative intensity value, and the average protein abundance of each group is calculated. The proteins with a difference multiple of >1.5 or <0.67 are differential proteins.

2.7 | Western blotting assay

After anesthetizing rats with 7% chloral hydrate, the rat lung tissue was fully lysed with lysis buffer (RIPA: PMSF = 100:1) to extract protein. Protein concentrations were determined using the BCA Protein Assay Kit (P0010; Beyotime, China). The antibodies of 20 target proteins were separated using sodium dodecyl sulfate–polyacrylamide gel electrophoresis (SDS–PAGE), then transferred to a nitrocellulose membrane, incubated with 5% skim milk for 1 h, and subsequently incubated with primary antibody at 4°C overnight. Goat anti-mouse IgG(H + L) labeled with horseradish peroxidase (A0216; 1:2000 dilution; Beyotime, China) and Goat anti-rabbit IgG(H + L) labeled with horseradish peroxidase were used as secondary antibodies (A0208; 1:1000 dilution; Beyotime, China). The fluorescence and chemiluminescence imaging equipment were utilized to detect the secondary antibody signal. Densitometry was used for protein band analysis.

2.8 | Quantitative real-time PCR (RT-PCR)

RT-PCR further verified the results of western blotting. After anesthetizing rats with 7% chloral hydrate, the lung tissues were taken, and total RNA samples were prepared using TRIzol (Ambion, USA). Total RNA (5 μL) was converted into cDNA using the PrimeScript™ RT (Takara Bio, Japan). The cDNA obtained was subjected to amplification using real-time PCR for 40–45 cycles. SYBR Premix Ex Taq™ II (Takara Bio, Japan) detected amplified product. The primers used in this study are listed in Table 1. The analysis of each sample was conducted in triplicate and afterward normalized to glyceraldehyde 3-phosphate dehydrogenase (GAPDH), serving as reference RNA. The relative expression levels were identified through the $2^{-\Delta\Delta Ct}$ technique.

2.9 | Statistical analyses

The DDA raw files were subjected to analysis through Proteome Discoverer (PD), v.2.2 (Thermo Fisher Scientific, USA), against the rat UniProt FASTA database. Datasets were processed through Statistical Package for the Social Sciences (SPSS), v.17.0. All data were expressed as mean ± standard deviation (SD), and each dot represents a biological replicate. For data with equal variances, the comparative analysis was conducted through one-way ANOVA; least significant difference (LSD) test was used for multiple comparisons of groups. For data with unequal variances, the rank sum test is used for comparative analysis; the Tamhane post-hoc test was used for multiple comparisons of groups; $p < .05$ was deemed to confer statistical significance.

3 | RESULTS

3.1 | Treatment of ECH in preventing HPH

Our research group has found in previous studies that ECH could prevent HPH by regulating pulmonary artery function and improving vascular remodeling.[12]

3.1.1 | Liquid chromatography–tandem mass spectrometry (LC–MS/MS) analysis

By analyzing the chronic hypoxia group, ECH group, and normoxia group, overall, 16 090 proteins were found. A total of 158 distinct proteins were recognized as differentially expressed within the chronic hypoxia group compared to the normoxia group by the proteomics analysis (Figure 3). It was also determined that 45 of these proteins were down-regulated, and 113 were up-regulated. When

TABLE 1 Primer sequences for quantitative real-time PCR.

Gene	Forward	Reverse
ACSL1	5′-TGTGGGGTGGAAATCATCGG-3′	5′-CATTGCTCCTTTGGGGTTGC-3′
COL6A1	5′-CTCGAGGGCTACAAGGAACC-3′	5′-AAATTGCGCCGGTATGTGTG-3′
COL4A2	5′-AGACAACAGATGACCCGCTG-3′	5′-GCGAAGTTGCAGACGTTGTT-3′
COL1A1	5′-CTGCTCGGTCGGGCTAC-3′	5′-GTTGCCTGGTTGTCCTTTGG-3′
PC	5′-GGCCATGCGCTTCTTGTATG-3′	5′-GGGTAGTTGGTGTAGCCCAC-3′
GAPDH	5′-CCTGCACCACCAACTGCTTA-3′	5′-CATCACGCCACAGCTTTCCA-3′

comparing the ECH group against the chronic hypoxia group, 106 differentially expressed proteins were observed (Figure 3). Of these proteins, it was found that 54 proteins showed up-regulation and 52 proteins were down-regulated.

We compared 20 proteins that were up-regulated in the hypoxia group and down-regulated in the ECH group or down-regulated in the hypoxia group and up-regulated in the ECH group. Table 2 displays the 20 differentially expressed proteins with clear functions in each group. Among the examined proteins, 1–19 exhibited up-regulation in the chronic hypoxia group (M/N difference multiple >1.5). Conversely, these proteins showed down-regulation in the ECH group (M/Y difference multiple >1.5). Protein 20 exhibited down-regulation in the chronic hypoxia group (M/N difference multiple <0.67), whereas it displayed up-regulation in the ECH group (M/Y difference <0.67).

FIGURE 3 Venn diagram highlighting quantities of differential proteins between the chronic hypoxia group (M) and normoxia group (N) as well as between the chronic hypoxia group and ECH group (Y).

3.1.2 | Western blotting verified the results of LC–MS/MS analysis

Western blotting further verified that there were significant differences in the expression of 5 proteins, which were in concordance with those obtained through LC–MS/MS analysis (Figure 4A). The Western blotting analysis confirmed that the levels of Acyl-CoA Synthetase Long-Chain Family Member 1 (ACSL1), Collagen alpha-1 (VI) chain (COL6A1), Collagen alpha-2 (IV) chain (COL4A2), Collagen alpha-1 (I) chain (COL1A1), and Pyruvate carboxylase (PC) were significantly higher in chronic hypoxia group compared against normoxia group ($^*p < .05$, $n = 3$) and in comparison the administration of ECH (30 mg/kg) resulted in a substantial decrease in the expression of the aforementioned proteins ($^*p < .05$, $n = 3$) compared to the chronic hypoxia group (Figure 4B–F).

TABLE 2 Twenty differentially expressed proteins in each group.

	Protein descriptions	Protein name	Gene	M/N	M/Y
1	Fatty acid-binding protein, adipocyte	FABP4_RAT	FABP4	13.9185	13.4227
2	Collagen alpha-1(I) chain	COL1A1_RAT	COL1A1	6.2294	4.5430
3	Long-chain-fatty-acid--CoA ligase 1	ACSL1_RAT	ACSL1	3.7757	4.0645
4	Fibrillin 1, isoform CRA_a	G3V9M6_RAT	FBN1	5.4515	3.3509
5	Microfibrillar-associated protein 2 (Predicted)	D3Z952_RAT	MFAP2	3.5527	3.1125
6	Pyruvate carboxylase, mitochondrial	PYC_RAT	PC	2.8167	2.5315
7	Asporin	Q5XIH1_RAT	ASPN	2.1082	2.3853
8	Procollagen, type VI, alpha 2, isoform CRA_a	F1LNH3_RAT	COL6A2	2.3333	2.2833
9	Protein Col4a2	F1M6Q3_RAT	COL4A2	3.9053	2.2726
10	NADP-dependent malic enzyme	MAOX_RAT	ME1	2.1558	2.2075
11	Protein COL6A1	D3ZUL3_RAT	COL6A1	2.3858	2.0336
12	Protein Itga2b	D3ZAC0_RAT	ITGA2B	1.5447	1.9913
13	Platelet factor 4	PLF4_RAT	PF4	1.5931	1.9715
14	Protein Col4a1	F1MA59_RAT	COL4A1	2.9694	1.8791
15	Arachidonate 12-lipoxygenase, 12S-type	ALOX12_RAT	ALOX12	2.7728	1.8760
16	Protein nephronectin	M0RAX9_RAT	NPNT	2.3878	1.7719
17	Coagulation factor XIII A chain	G3V811_RAT	F13A1	1.7695	1.74
18	Protein Col6a5	F1LZF4_RAT	COL6A5	1.5058	1.5971
19	Fibrinogen-like 2	G3V7P2_RAT	FGL2	1.5050	1.5695
20	Ig gamma-2B chain C region	IgG2b_RAT	IGH-1A	0.5068	0.5923

Abbreviations: M, Model group; N, Control group; Y, ECH group.

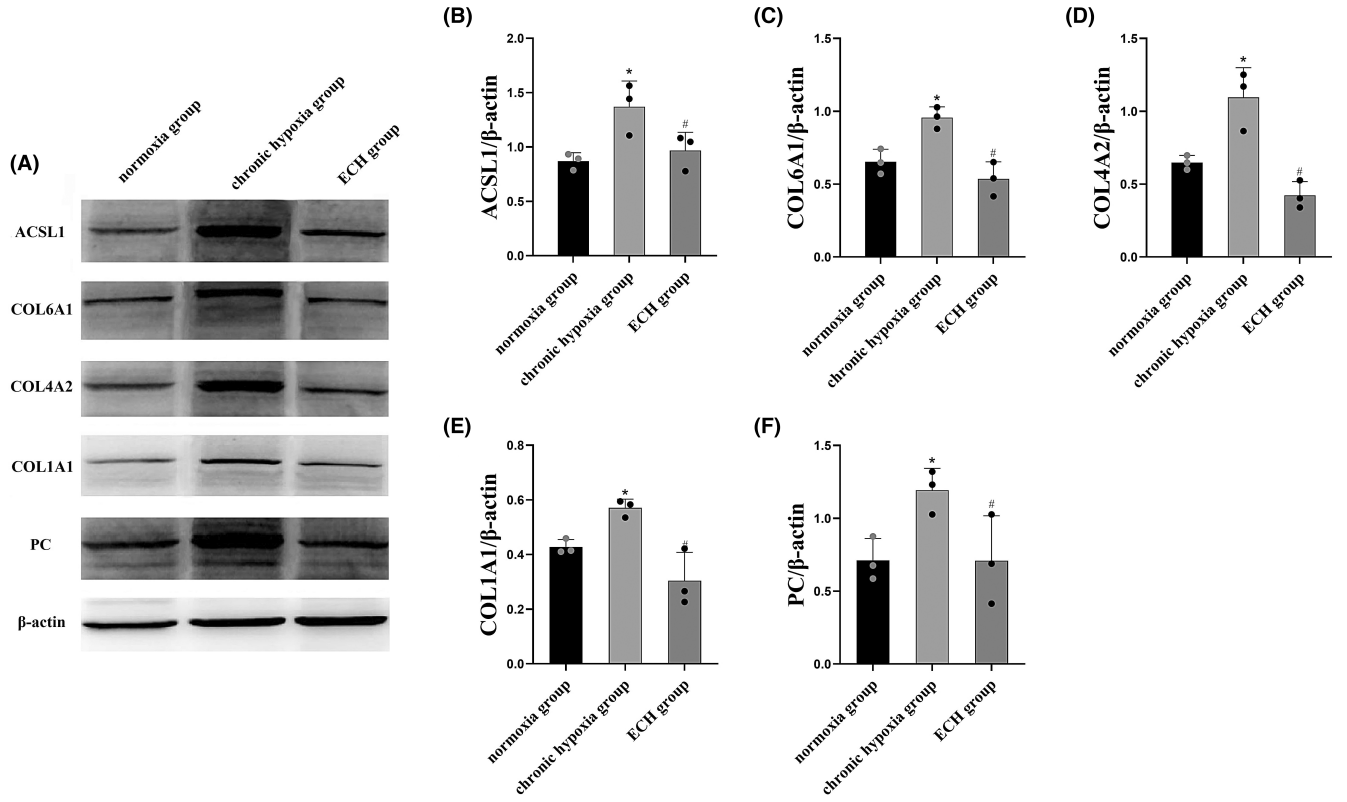

FIGURE 4 Effects of hypoxia and ECH on differential proteins expression. B, C, D, E, and F were the quantitative results of A. All data were expressed as mean ± standard deviation (SD), and each dot represents a biological replicate. For data with equal variances, the comparative analysis was conducted through one-way ANOVA; the least significant difference (LSD) test was used for multiple comparisons of groups. For data with unequal variances, the rank sum test is used for comparative analysis; the Tamhane post-hoc test was used for multiple comparisons of groups. $^{*}p < .05$ versus Normoxia group, $^{\#}p < .05$ versus Chronic hypoxia group, $n = 3$ (biological replicates).

3.1.3 | RT-PCR verified the outcomes of LC–MS/MS analysis

In comparison with the normoxia group, the chronic hypoxia group's mRNA expression levels for ACSL1, COL6A1, COL4A2, and PC were observed to be higher ($^{*}p < .05$, $n = 3$) (Figure 5). Additionally, the ECH treatment group (30 mg/kg) substantially decreased the mRNA expression levels of ACSL1, COL6A1, COL4A2, and PC in comparison against the chronic hypoxia group ($^{*}p < .05$, $n = 3$) (Figure 5A–C,E). In the aforementioned findings, except for COL1A1, the mRNA expression levels of the other components are coherent with the protein expression levels (Figure 5D).

3.2 | Treatment of ECH in treating HPH

The mPAP of normoxia group rats was 17.44 ± 1.95 mmHg. The mPAP of chronic hypoxia group rats increased to 41.23 ± 3.63 mmHg, and it has a significant difference compared with the normoxia group ($^{*}p < .05$) (Figure 6A). The RVHI was 0.21 ± 0.03 in the normoxia group and increased to 0.46 ± 0.03 in the chronic hypoxia group, with a significant difference compared with the normoxia group ($^{*}p < 0.05$) (Figure 6B). Besides, Hb, Hct, and RBC were 133.6 ± 11.14 g/L, 46.16 ± 2.36%, 7.34 ± 0.32 10^{12}/L and increased to 258.6 ± 8.08 g/L, 66.44 ± 2.37%, and 10.76 ± 0.38 10^{12}/L in chronic hypoxia group, with significant difference compared with normoxia group (all $^{*}p < 0.05$) (Figure 6C–E). These results indicated that the HPH rat model was successfully executed.

The mPAP was dropped to 34.52 ± 3.09, 28.13 ± 2.48, and 30.78 ± 3.64 mmHg, respectively, in the ECH group (10 mg/kg), ECH group (20 mg/kg), and ECH group (40 mg/kg) (compared with that in the chronic hypoxia group, both $^{\#}p < 0.05$) (Figure 6A). In addition, ECH (10 mg/kg) reduced Hb and Hct in HPH rats to 244.9 ± 14.15 g/L and 59.92 ± 1.84%, respectively, and ECH group (20 mg/kg) and ECH group (40 mg/kg) can also reduce Hb and Hct in rats (compared with the values in the chronic hypoxia group, $^{\#}p < .05$) (Figure 5C,D). The RVHI was dropped to 0.36 ± 0.03 in the ECH group (40 mg/kg) (compared with that in the chronic hypoxia group, $^{\#}p < .05$) (Figure 6B). These results show that ECH can improve HPH by reducing mPAP, Hb, Hct, and RVHI in rats.

HE staining of lung tissues showed that compared with the normoxia group, the pulmonary artery in the chronic hypoxia group was thickened and showed the characteristics of pulmonary artery remodeling (Figure 7A,B). After ECH (40 mg/kg) treatment, the above situation was alleviated (Figure 7C). The mean WT%, WA%, and LA% in chronic hypoxia group were 56.17 ± 3.73%,

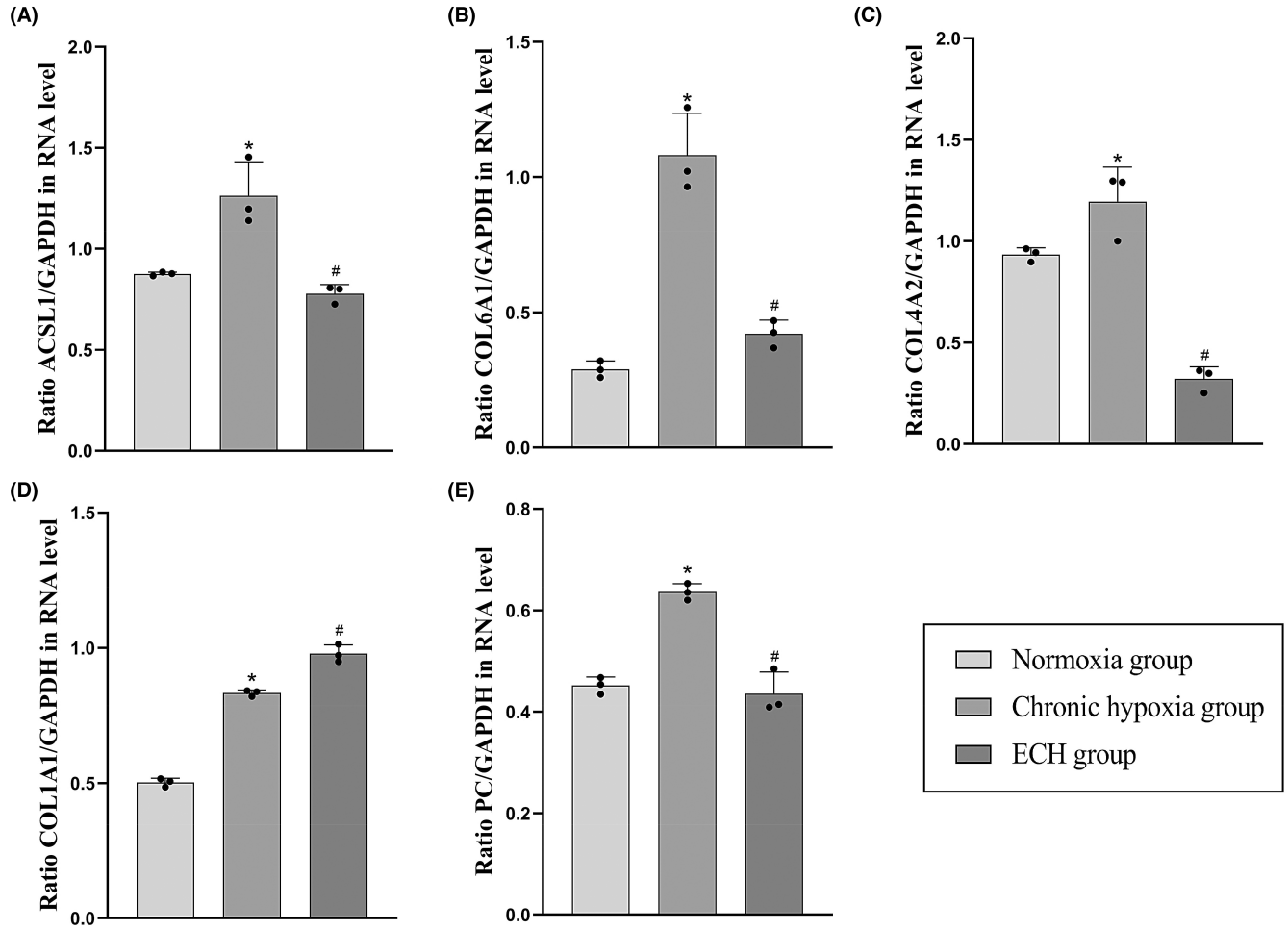

FIGURE 5 Changes of mRNA expression of differential proteins ACSL1 (A), COL6A1 (B), COL4A2 (C), COL1A1 (D), and PC (E) in three groups. All data were expressed as mean ± standard deviation (SD), and each dot represents a biological replicate. For data with equal variances, the comparative analysis was conducted through one-way ANOVA; the least significant difference (LSD) test was used for multiple comparisons of groups. For data with unequal variances, the rank sum test is used for comparative analysis; the Tamhane post-hoc test was used for multiple comparisons of groups. $^{*}p < .05$ versus Normoxia group, $^{\#}p < .05$ versus Chronic hypoxia group, $n = 3$ (biological replicates).

60.21 ± 4.67%, and 39.79 ± 4.67%, respectively. The WT% and WA% were significantly increased compared with the values in the normoxia group ($^{*}p < .05$), and the LA% was decreased compared with the normoxia group ($^{*}p < .05$). In the ECH (40 mg/kg) group, the mean WT%, WA%, and LA% were 36.12 ± 3.16%, 49.99 ± 3.12%, and 50.01 ± 3.12%, respectively. The WT% and WA% were significantly decreased compared with the chronic hypoxia group ($^{\#}p < .05$), and the LA% was increased compared with chronic hypoxia group ($^{\#}p < .05$) (Figure 7). These results show that ECH can alleviate pulmonary artery thickening and reverse pulmonary artery remodeling caused by hypoxia.

4 | DISCUSSION

In our previous study, we determined the preventive effect of ECH on HPH, but its specific mechanism was not clear.[9,12] In the clinic, it is generally after hypoxia and the development of corresponding symptoms that the use of drugs is considered. Some studies have found that rats exhibit basic symptoms of hypoxic pulmonary hypertension after being exposed to a low-pressure oxygen chamber simulating an altitude of 5000 m for 7 days. The average pulmonary artery pressure and right ventricular hypertrophy index of rats are significantly increased. The middle layer of the pulmonary artery is noticeably thickened, and there is an increase in extracellular matrix components.[13,14] At present, whether ECH has a therapeutic effect on HPH is still uncertain. Therefore, in this study, we applied a therapeutic administration method (ECH was given to rats after 7 days of hypoxia). The results showed that ECH (10, 20, and 40 mg/kg) had a therapeutic effect on HPH, among which 40 mg/kg had the best effect. At the same time, the mechanism of ECH in preventing HPH was preliminarily discussed by label-free quantitative proteomic analysis.

The current research seamlessly integrated many cutting-edge methodologies, such as enzyme digestion, protein extraction, bioinformatics analysis, and LC–MS/MS, to conduct quantitative

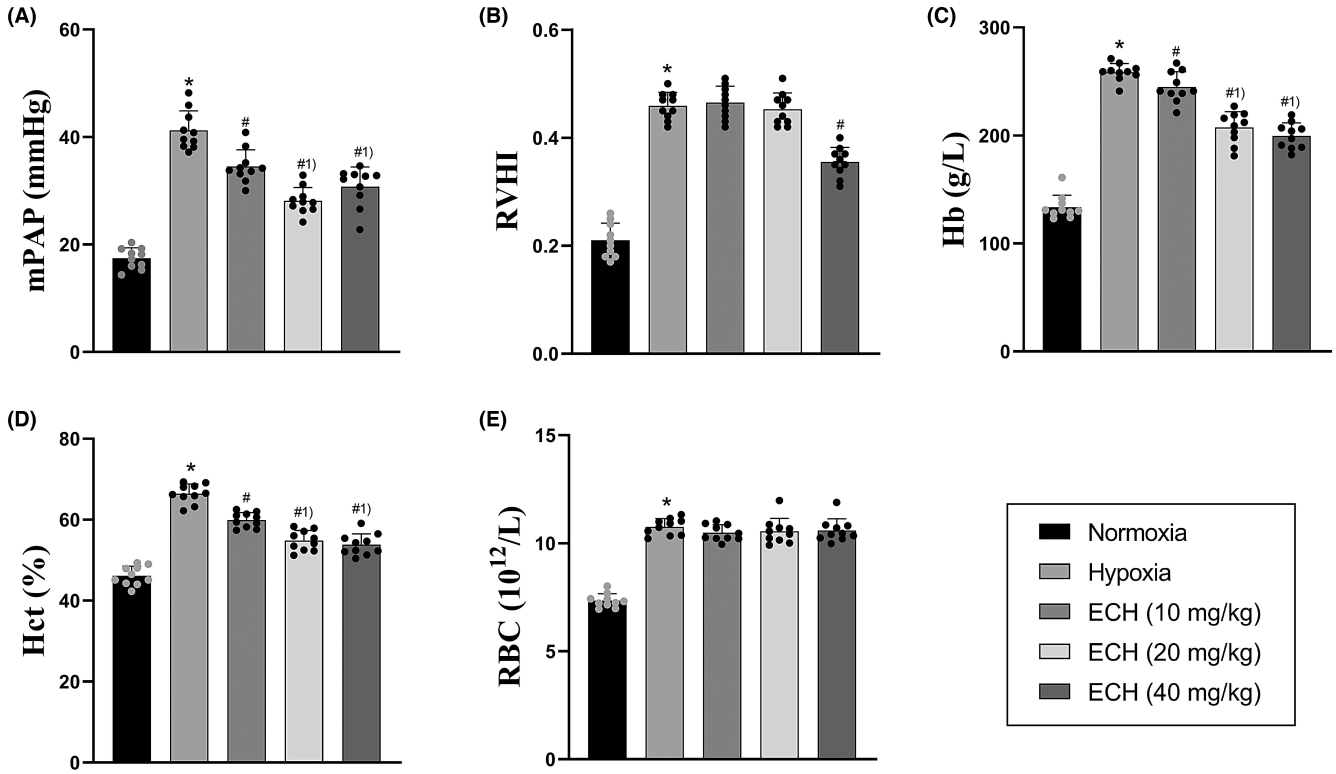

FIGURE 6 Effect of ECH on mPAP (A), RVHI (B), Hb (C), Hct (D), and RBC (E). All data were expressed as mean ± standard deviation (SD), and each dot represents a biological replicate. For data with equal variances, the comparative analysis was conducted through one-way ANOVA; the least significant difference (LSD) test was used for multiple comparisons of groups. For data with unequal variances, the rank sum test is used for comparative analysis; the Tamhane post-hoc test was used for multiple comparisons of groups. $^{*}p < .05$ versus normoxia, $^{\#}p < .05$ versus hypoxia,[1] $p < .05$ versus ECH (10 mg/kg), $n = 10$ (biological replicates).

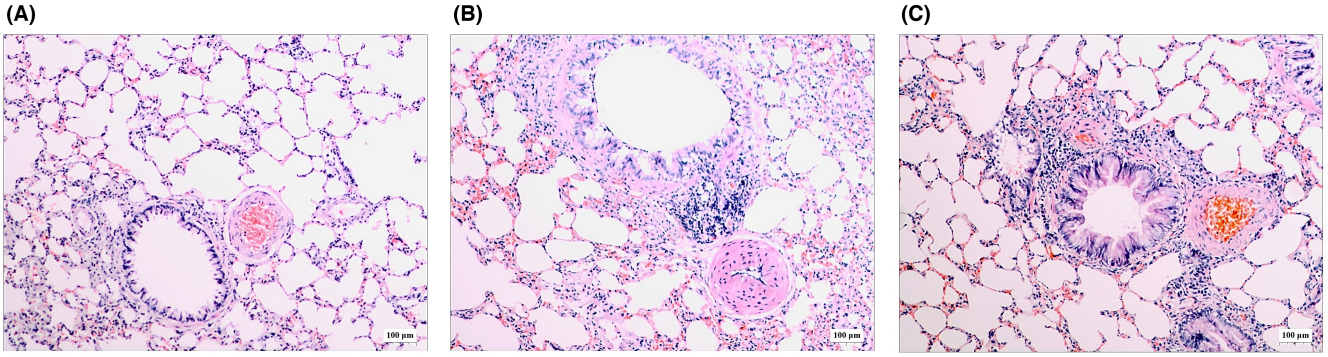

FIGURE 7 Representative HE staining of the lung tissues in each group. (A) normoxia group; (B) chronic hypoxia group; and (C) ECH (40 mg/kg) group. The scale bar represents 100 μm. All data were expressed as mean ± standard deviation (SD), and each dot represents a biological replicate. For data with equal variances, the comparative analysis was conducted through one-way ANOVA; the least significant difference (LSD) test was used for multiple comparisons of groups. For data with unequal variances, the rank sum test is used for comparative analysis; the Tamhane post-hoc test was used for multiple comparisons of groups. $^{*}p < .05$ versus normoxia group, $^{\#}p < .05$ versus chronic hypoxia group, $n = 11$ (biological replicates).

proteomic investigations on the samples under study. Using a label-free quantification technique, this investigation identified 16 090 proteins in each of the three groups. A total of 5 proteins exhibiting differential expression were screened across three distinct groups.

The presence of perivascular inflammation is a notable pathogenic characteristic observed in the majority of animal models utilized to study pulmonary hypertension (PH).[15] The nuclear factor-κB (NF-κB) triggers expression for several proinflammatory genes. ACSL1, operates upstream of the NF-κB pathway and is essential for activating NF-κB, mediated through tumor necrosis factor-α. Hence, the up-regulation of ACSL1 expression might potentially exacerbate the perivascular inflammatory response through the augmentation of proinflammatory gene expression.[16]

There are similarities in the etiology of cancer and PH, mainly regarding an increase in cell proliferation, oxidative stress, and having an anti-apoptosis effect.[17,18] Vascular remodeling is a prominent pathogenic characteristic observed in the progression of HPH. Several factors, including oxidative stress, endothelial dysfunction, extracellular matrix (ECM) deposition, and excessive cell proliferation, have been identified as contributors to this process of vascular remodeling.[2,19–21] The administration of a PC inhibitor has been shown to have a notable impact on many physiological parameters in sugen/hypoxia rats. Specifically, it leads to a considerable reduction in right ventricular systolic pressure, Fulton index, cell proliferation, and vascular proliferation. As a result, this intervention effectively improves pulmonary vascular remodeling and alleviates PH within such animal models.[22] Collagen VI mainly includes three genes, COL6A1, COL6A2, and COL6A3, which can promote cell proliferation, migration, adhesion, and survival in many cell types.[23] The expression of Matrix Metalloproteinase-2 and Matrix Metalloproteinase-9 is crucial in the control of vascular smooth muscle cell proliferation and migration. The decrease in matrix metalloproteinase-2 and matrix metalloproteinase-9 expression can be attributed to the down-regulation of COL6A1 in vascular smooth muscle cells.[24] In mice with hypoxia-induced PH, fibroblasts undergo differentiation into myofibroblasts. Subsequently, myofibroblasts migrate from the adventitia to the medial and intima layers of the pulmonary artery. This migration process results in the up-regulation of specific collagen genes, namely COL1A1, COL6A1, COL6A2, COL4A1, and COL4A2. Consequently, ECM protein expression increases, facilitating pulmonary artery remodeling.[24–28]

In brief, it has been observed that ECH possesses the ability to inhibit the inflammatory response and prolong the progression of HPH by modulating the expression of ACSL1 proteins in a down-regulatory manner. The upregulation of PC protein in the rat model of HPH potentially facilitates the growth and proliferation of smooth muscle cells. Conversely, the administration of ECH may have inhibitory effects on the expression of the aforementioned proteins. The administration of ECH can potentially suppress the process of pulmonary vascular remodeling through its ability to decrease the accumulation of certain collagen family members, including COL6A1, COL4A2, and COL1A1.

5 | CONCLUSION

This study suggests that ECH could represent a potential therapeutic agent for HPH; unbiased proteomic analysis suggests that it may exert its effects in preclinical models through modulation of inflammatory pathways, extracellular matrix accumulation, and oxidative stress.

AUTHOR CONTRIBUTIONS

Conceptualization: Xiangyun Gai. *Data curation*: Xiangyun Gai and Qingqing Xia. *Investigation*: Hongmai Wang, Hongtao Bi, Jinyu Wang, and Yuefu Zhao. *Methodology*: Xiangyun Gai. *Writing—original draft*: Qingqing Xia and Hongmai Wang. *Writing—review and editing*: Xiangyun Gai, Qingqing Xia, and HMW.

ACKNOWLEDGMENTS

We express our gratitude to the Qinghai Provincial Key Laboratory of Tibetan Medicine Pharmacology and Safety Evaluation of the Northwest Institute of Plateau Biology of the Chinese Academy of Science.

FUNDING INFORMATION

This work was supported by the Application Foundation Project grant of Qinghai Province, China (2020-ZJ-703) and Kunlun Talents and High-level Innovative Entrepreneurship Program of Qinghai Province (2020).

CONFLICT OF INTEREST STATEMENT

The authors declare that they have no competing interests.

DATA AVAILABILITY STATEMENT

The data that support the findings of this study are available on request from the corresponding author.

ETHICS STATEMENT

All the experimental procedures were approved by the Experimental Animal Welfare Ethics Review Committee of the Northwest Institute of Plateau Biology, Chinese Academy of Sciences [No. 2023-19] and all animals were treated in accordance with the Guide for the Care and Use of Laboratory Animals.

ORCID

Xiangyun Gai https://orcid.org/0009-0006-8441-9715
Qingqing Xia https://orcid.org/0009-0004-8876-0414
Hongmai Wang https://orcid.org/0009-0008-6095-7943
Hongtao Bi https://orcid.org/0000-0002-5569-8552
Jinyu Wang https://orcid.org/0009-0006-8441-9715
Yuefu Zhao https://orcid.org/0009-0009-4414-857X

REFERENCES

1. Liu R, Xu C, Zhang W, et al. FUNDC1-mediated mitophagy and HIF1α activation drives pulmonary hypertension during hypoxia. *Cell Death Dis*. 2022;13:634.
2. Veith C, Vartürk-Özcan I, Wujak M, et al. SPARC, a novel regulator of vascular cell function in pulmonary hypertension. *Circulation*. 2022;145:916-933.
3. Humbert M, Kovacs G, Hoeper MM, et al. 2022 ESC/ERS guidelines for the diagnosis and treatment of pulmonary hypertension. *Eur Heart J*. 2022;43:3618-3731.
4. Ruopp NF, Cockrill BA. Diagnosis and treatment of pulmonary arterial hypertension: a review. *JAMA*. 2022;327:1379.
5. Zeng KW, Wang JK, Wang LC, et al. Small molecule induces mitochondrial fusion for neuroprotection via targeting CK2 without affecting its conventional kinase activity. *Sig Transduct Targrt Ther*. 2021;6:71.
6. Zhou L, Yao M, Tian Z, et al. Echinacoside attenuates inflammatory response in a rat model of cervical spondylotic myelopathy via inhibition of excessive mitochondrial fission. *Free Radic Biol Med*. 2020;152:697-714.
7. Ye Y, Song Y, Zhuang J, Wang G, Ni J, Xia W. Anticancer effects of echinacoside in hepatocellular carcinoma mouse model and HepG2 cells. *J Cell Physiol*. 2019;234:1880-1888.
8. Gai XY, Tang F, Ma J, et al. Antiproliferative effect of echinacoside on rat pulmonary artery smooth muscle cells under hypoxia. *J Pharmacol Sci*. 2014;126:155-163.
9. Gai XY, Wei YH, Zhang W, et al. Echinacoside induces rat pulmonary artery vasorelaxation by openi-ng the NO-cGMP-PKG-BK_{Ca} channels and reducing intracellular Ca^{2+} levels. *Acta Pharmacol Sin*. 2015;36:587-596.
10. Fu J, Yang Q, Luo Y, et al. Label-free proteome quantification and evaluation. *Brief Bioinform*. 2023;24:bbac477.
11. Letunica N, Van Den Helm S, McCafferty C, et al. Proteomics in thrombosis and hemostasis. *Thr- Omb Haemostasis*. 2022;122:1076-1084.
12. Gai XY, Lin PC, He YF, et al. Echinacoside prevents hypoxic pulmonary hypertension by regulating the pulmonary artery function. *J Pharmacol Sci*. 2020;144:237-244.
13. Wu KJ, Yan YS, Liu BC, et al. Alternations of collagen content and collagen gene expression in rat vascular structural remodeling of pulmonary artery induced by hypoxia. *Chin J Tuberc Respir Dis*. 1994;17:152-155.
14. Ma L, Liu CC, Zhou Z, et al. Construction of pulmonary vascular remodeling model of hypoxic pulmonary hypertension in rats and the expression of MicroRNA-34a in lung tissue. *Chin High Alt Med Biol*. 2018;39:6-12.
15. Price LC, Wort SJ, Perros F, et al. Inflammation in pulmonary arterial hypertension. *Chest*. 2012;141:210-221.
16. Al-Rashed F, Ahmad Z, Iskandar MA, et al. TNF-α induces a proinflammatory phenotypic shift in monocytes through ACSL1: relevance to metabolic inflammation. *Cell Physiol Biochem*. 2019;52:397-407.
17. Pullamsetti SS, Savai R, Seeger W, Goncharova EA. Translational advances in the field of pulmonary Hyperte-nsion. From cancer biology to new pulmonary arterial hypertension therapeutics. Targeting cell growth and proliferation signaling hubs. *Am J Resp Crit Care*. 2017;195:425-437.
18. Rhodes CJ. The cancer hypothesis of pulmonary arterial hypertension: are polyamines the new war-burg? *Eur Respir J*. 2020;56:2002350.
19. Xu T, Liu S, Ma T, Jia Z, Zhang Z, Wang A. Aldehyde dehydrogenase 2 protects against oxidative stress associated with pulmonary arterial hypertension. *Redox Biol*. 2017;11:286-296.
20. Evans CE, Cober ND, Dai Z, Stewart DJ, Zhao YY. Endothelial cells in the pathogenesis of pulmonary arterial hypertension. *Eur Respir J*. 2021;58:2003957.
21. Jandl K, Radic N, Zeder K, Kovacs G, Kwapiszewska G. Pulmonary vascular fibrosis in pulmonary hypertension-the role of the extracellular matrix as a therapeutic target. *Pharmacol Therapeut*. 2023;247:108438.
22. Valuparampil Varghese M, James J, Eccles CA, Niihori M, Rafikova O, Rafikov R. Inhibition of Anaplerosis attenuated vascular proliferation in pulmonary arterial hypertension. *J Clin Med*. 2020;9:443.
23. Bönnemann CG. The collagen VI-related myopathies: muscle meets its matrix. *Nat Rev Neurol*. 2011;7:379-390.
24. Chen Z, Wu Q, Yan C, du J. COL6A1 knockdown suppresses cell proliferation and migration in human aortic vascular smooth muscle cells. *Exp Ther Med*. 2019;18:1977-1984.
25. Urushiyama H, Terasaki Y, Nagasaka S, et al. Role of α1 and α2 chains of type IV collagen in early fibrotic lesions of idiopathic interstitial pneumonias and migration of lung fibroblasts. *Lab Investig*. 2015;95:872-885.
26. Sen P, Dharmadhikari AV, Majewski T, et al. Comparative analyses of lung transcriptomes in patien-ts with alveolar capillary dysplasia with misalignment of pulmonary veins and in foxf1 heterozygous knockout mice. *PLoS One*. 2014;9:e94390.
27. Zhang S, Yin Z, Qin W, et al. Pirfenidone inhibits hypoxic pulmonary hypertension through the NADPH/ROS/p38 pathway in adventitial fibroblasts in the pulmonary artery. *Mediat Inflamm*. 2020;2020:2604967.
28. Loscertales M, Nicolaou F, Jeanne M, et al. Type IV collagen drives alveolar epithelial-endothelial association and the morphogenetic movements of septation. *BMC Biol*. 2016;14:59.

How to cite this article: Gai X, Xia Q, Wang H, Bi H, Wang J, Zhao Y. Study on the mechanism of echinacoside in preventing and treating hypoxic pulmonary hypertension based on proteomic analyses. *Pharmacol Res Perspect*. 2024;12:e70025. doi:10.1002/prp2.70025